Mesoscale Monitoring of Soil Moisture across a Statewide Network

BRADLEY G. ILLSTON,* JEFFREY B. BASARA,* DANIEL K. FISHER,+ RONALD ELLIOTT,#
CHRISTOPHER A. FIEBRICH,* KENNETH C. CRAWFORD,* KAREN HUMES,@ AND ERIC HUNT*

*Oklahoma Climatological Survey, University of Oklahoma, Norman, Oklahoma
+ USDA-ARS, Stoneville, Missouri
# Oklahoma State University, Oklahoma City, Oklahoma
@ University of Idaho, Boise, Idaho

(Manuscript received 13 February 2007, in final form 22 June 2007)

ABSTRACT

Soil moisture is an important component in many hydrologic and land–atmosphere interactions. Understanding the spatial and temporal nature of soil moisture on the mesoscale is vital to determine the influence that land surface processes have on the atmosphere. Recognizing the need for improved in situ soil moisture measurements, the Oklahoma Mesonet, an automated network of 116 remote meteorological stations across Oklahoma, installed Campbell Scientific 229-L devices to measure soil moisture conditions. Herein, background information on the soil moisture measurements, the technical design of the soil moisture network embedded within the Oklahoma Mesonet, and the quality assurance (QA) techniques applied to the observations are provided. This project also demonstrated the importance of operational QA regarding the data collected, whereby the percentage of observations that passed the QA procedures increased significantly once daily QA was applied.

1. Introduction

Soil moisture is an important component in many hydrologic and land–atmosphere interactions. Anomalous soil moisture conditions on a large scale can lead to droughts or floods (Delworth and Manabe 1989, 1993), while regional variations can impact the development of the planetary boundary layer (Zdunkowski et al. 1975; Betts and Ball 1995), the formation of low-level boundaries or land breezes (Enger and Tjernstrom 1991; Segal and Arritt 1992), convective initiation (Lanicci et al. 1987; Segal et al. 1995), and precipitation recycling (Anthes 1984; Brubaker et al. 1993; Brubaker and Entekhabi 1996). Furthermore, the relative partitioning between latent and sensible heat fluxes at all spatial and temporal scales is controlled largely by variations in soil moisture conditions. Thus, understanding the spatial and temporal nature of soil moisture on the mesoscale is vital to determine the influence that land surface processes have on the atmosphere.

The need for continuous, automated soil moisture observations has been addressed in articles such as Emanuel et al. (1995), who emphasized that improved observations of soil moisture conditions may lead to dramatic forecasting improvements. These scientists found that soil moisture observations can add value to predictions of the location and timing of the onset of deep convection over land, quantitative precipitation forecasting, and seasonal climate prediction. Furthermore, Entekhabi et al. (1999) noted that existing mesoscale surface networks could be enhanced with sensors to measure soil water as well as atmospheric processes. The information gathered by these collocated sensors could be used to evaluate new hydrological theories, modeling, and remote sensing techniques.

Recognizing the need for improved in situ measurements, the Oklahoma Mesonetwork (Mesonet; Brock et al. 1995; McPherson et al. 2007), an automated network of 116 remote meteorological stations across Oklahoma, installed sensing devices to measure soil moisture conditions. Because the need for soil moisture observations in Oklahoma extended beyond the scientific community to potential customers focused on agriculture, water resources, and natural resource policy, Oklahoma Mesonet scientists designed the soil mois-

Corresponding author address: Bradley G. Illston, Oklahoma Climatological Survey, 120 David L. Boren Blvd., Suite 2900, Norman, OK 73072-7305.
E-mail: illston@ou.edu

DOI: 10.1175/2007JTECHA993.1

ture network to meet as many needs as possible without sacrificing data quality. This paper provides background information on the soil moisture measurements, the technical design of the soil moisture network embedded within the Oklahoma Mesonet, and the quality assurance (QA) techniques applied to the observations.

2. History of the soil moisture network

The Oklahoma Mesonetwork began in 1991 as a statewide mesoscale environmental monitoring network (Brock et al. 1995; McPherson et al. 2007) with at least one site in each of Oklahoma's 77 counties. In 1996, with support from the National Science Foundation (NSF), the Mesonet deployed soil moisture sensors at 60 sites at four different depths, where possible: 5, 25, 60, and 75 cm below the surface. Soil moisture data are collected every 30 min and recorded locally at each site. A central ingest system at the Oklahoma Climatological Survey (OCS) at the University of Oklahoma remotely collects the data every 30 min.

The soil moisture sensor installed at Oklahoma Mesonet sites, described in section 3a, is a heat-dissipation sensor manufactured by Campbell Scientific, Incorporated (CSI). This particular sensor was also installed in two other networks in the Southern Great Plains: the Department of Energy's Atmospheric Radiation Measurement (DOE ARM) network (Schneider et al. 2003) and the U.S. Department of Agriculture/Agricultural Research Service (USDA/ARS) network (Starks 1999). The DOE ARM network extends into Kansas while the dense USDA/ARS network is nested within the Oklahoma Mesonet. Together, the three networks offer an opportunity to examine spatial scaling aspects of soil moisture climatology for both short and long periods of time.

Before installing sensors during 1996–97, Mesonet personnel considered a number of criteria to select the site locations. Because the 60 sites represented a subset of the Oklahoma Mesonet, Mesonet personnel desired an even spatial distribution to ensure statewide coverage of soil moisture monitoring. Additional considerations included soil conditions at each site (especially depth to rock, or history of soil disturbance) and the existence of 2-m wind speed data at the site [used to estimate evapotranspiration (ET)].

In 1999, Mesonet personnel augmented an additional subset of Mesonet stations with a suite of instruments capable of measuring surface heat fluxes and components of the radiation budget. Technicians installed the sensors at Mesonet sites during 1999 (and very early 2000) as part of the Oklahoma Atmospheric Surface-Layer Instrumentation System Project (OASIS; Basara and Crawford 2002) with support obtained via a major research infrastructure grant provided by the NSF. Because soil moisture was a key component of the ground heat flux measurement, technicians added soil moisture sensors to 42 additional sites during 1999 at the 5- and 25-cm depths.

In addition to the major installations (discussed above), Mesonet technicians have installed soil moisture sensors at six additional sites since 2000 and have decommissioned the sensors at five sites. As of January 2007, the Oklahoma Mesonet includes soil moisture sensors at a depth of 5 cm at 103 sites, 25-cm sensors at 101 sites, 60-cm sensors at 76 sites, and 75-cm sensors at 53 sites. The current deployment of soil moisture sensors at Oklahoma Mesonet sites is displayed in Fig. 1.

3. Network design

a. The Campbell Scientific 229-L sensor

The soil moisture sensor installed at Oklahoma Mesonet sites is the CSI 229-L heat-dissipation sensor. Mesonet scientists chose this sensor over other soil moisture sensors because of its ease of use, minimal soil disturbance during installation, small size (which allowed for installation at multiple independent depths), ease of automation, and absence of potentially harmful radiation (i.e., as compared to neutron probe measurements; Basara 1998).

The 229-L sensor's (Fig. 2) body shape is a right cylinder with a length of 60 mm and a diameter of 14 mm. A ceramic matrix, which is composed of 32 mm of the sensor length, surrounds a hypodermic needle. The water-adsorbing characteristics of the matrix are similar to those of a silt loam soil, so the ceramic matrix wets and dries on time scales similar to most soils, except for those with high sand fractions. The needle contains a copper–constantan thermocouple and a resistor that ranges from 32.5 to 33.5 ohms. Three copper wires and one constantan wire reside in a shielded burial-grade sheath to connect with the datalogger.

During operation, the 229-L sensor measures a temperature difference (ΔT_{sensor}), which is calculated as the change in sensor temperature after a heat pulse is introduced (Basara and Crawford 2000). First, the thermocouple measures an initial temperature. Next, a 50-mA current passes through the resistor for 21 s. Immediately after the current ceases, the thermocouple measures a final temperature value. The difference between the initial and final temperature measurements is designated as the temperature difference of the sensor (ΔT_{sensor}). The magnitude of heat dissipation varies as a function of the sensor's specific heat and thermal conductivity. Thus, a constant interval of heating leads to

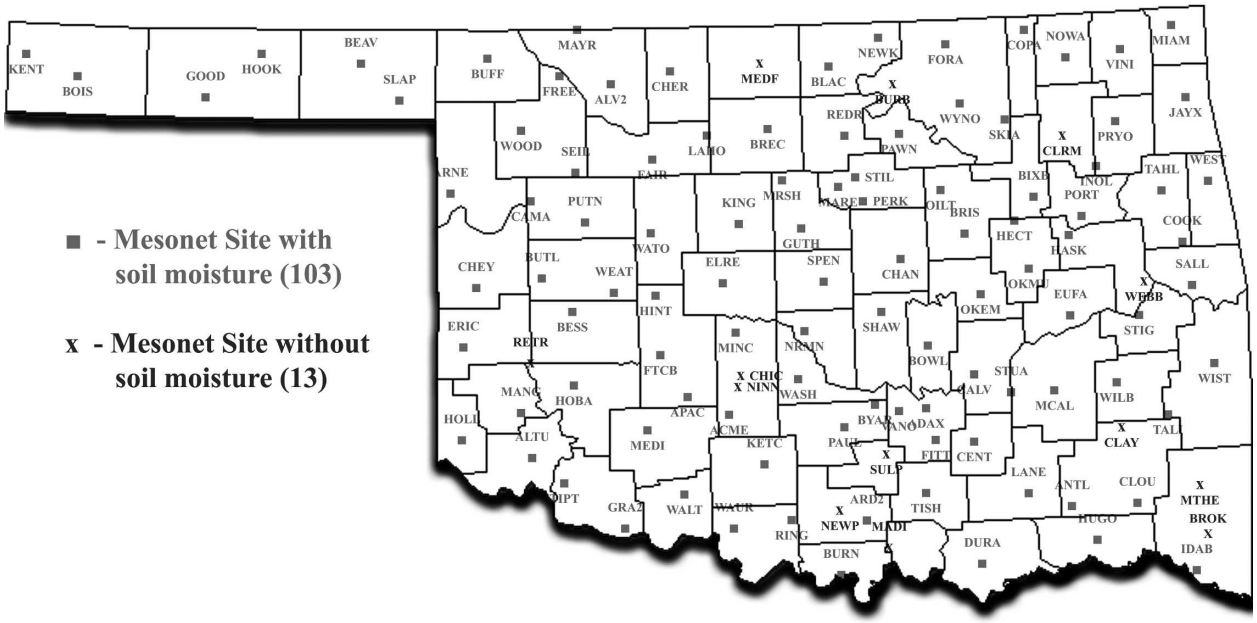

FIG. 1. Locations of Oklahoma Mesonet sites with soil moisture sensors in 2007.

different temperature rises depending on the water content of the sensor (the water potential of the sensor is assumed to be in equilibrium with that of the soil). Because of this measurement principal, the 229-L sensor does not return useful values during frozen soil conditions.

b. Installation procedures

1) LABORATORY CALIBRATION

Laboratory personnel inventory each Campbell Scientific 229-L soil moisture sensor in the Mesonet database as soon as it arrives from the manufacturer. The laboratory calibration is needed to identify and remove the inherent sensor-to-sensor variability caused by slight differences in the resistance heater, which ranges between 32.5 and 33.5 ohms. To begin the calibration procedure, technicians connect each sensor to a datalogger and multiplexer (mux) identical to those installed at Mesonet sites. Next, technicians measure and record the resistance of the thermocouple circuit and the heating element circuit. These resistance values can be used to troubleshoot problems associated with suspect data from installed sensors. As such, field measurements of the resistance values can be compared to laboratory values to determine whether errors are from the soil moisture sensors or from other peripheral equipment.

Next, the technician places the sensor into a bag along with DRIERITE desiccant for 3–4 days to remove the majority of residual moisture within the sensor. During this time, a datalogger records data every 15 min and calculates the largest temperature difference (ΔT_{max}) from the period. Technicians then place the sensor in a beaker of distilled water and jostle the sensor to remove as many air bubbles as possible from its porous ceramic matrix. Likewise, a datalogger records the sensor's observations for 3–4 days. Thus,

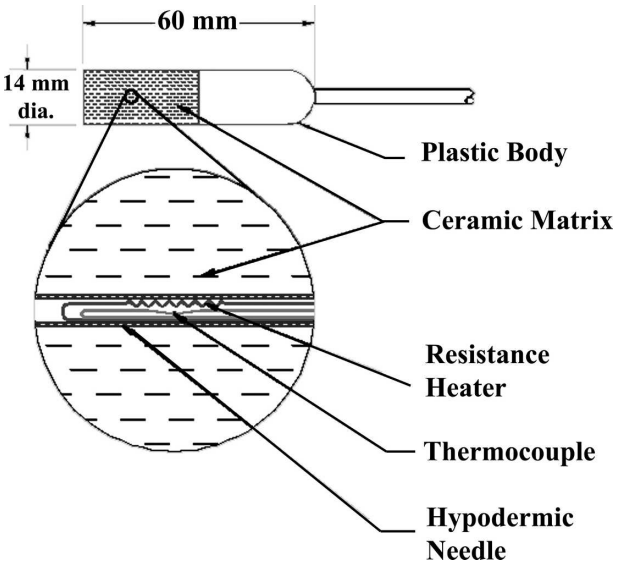

FIG. 2. The Campbell Scientific 229-L sensor.

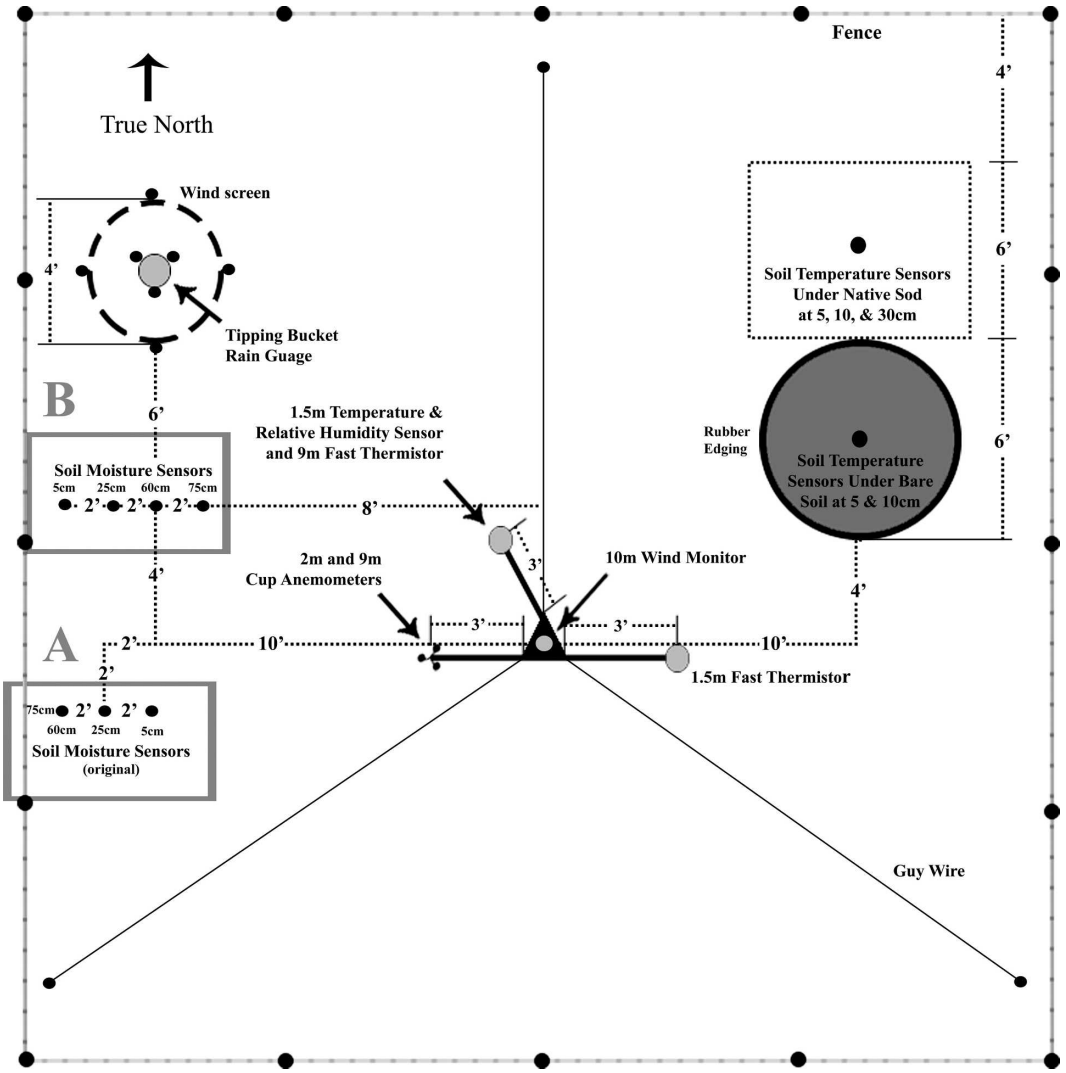

FIG. 3. Overhead view of a Mesonet station indicating the 229-L sensor locations with (a) the original installation locations and (b) the current installation locations.

the smallest temperature difference value ($\Delta T_{\min}$) is recorded. Finally, the technician removes the sensor from the distilled water, allows it to dry for 3–4 days on paper towels, and wraps it in antistatic foam for protection during transport to the field.

2) FIELD INSTALLATION

Technicians installed each soil moisture sensor using one of two methods at Mesonet sites. First, technicians dug a shallow trench 3.7 m westward from the Mesonet tower and 1.2 m northward. Trenches were deep enough to house all wires in conduit beneath the surface. Then, technicians used a posthole digger to create holes that were 10 cm in diameter and aligned east–west (Fig. 3). The original installation method (Method A) has sensors in three separate holes (5, 25, and 60/75 cm deep); the current installation method (Method B) has sensors in four separate holes (5, 25, 60, and 75 cm deep). As technicians dug each hole, they carefully placed the removed soil in consecutive piles on a tarp so that they could return the soil into the hole with the same initial stratification. Additionally, technicians removed the top few inches of soil with all vegetation intact to be replaced upon completion of the sensor installation. This methodology minimally disturbed the soil environment of the installed sensors.

Along the southern wall of each hole, technicians removed a horizontal core, 10 cm long and 14 mm in diameter (the same dimensions as the 229-L sensor), from the correct depth below the surface (i.e., either 5, 25, 60, or 75 cm). For the original installation method, technicians installed the 75-cm sensor on the western

wall of the westernmost hole. Field technicians sealed half of each core in a container and sent the soil core for soil analysis. Then they mixed the other half of each core with water to create a slurry and inserted a portion of the slurry into the hole. The slurry helps to promote contact between the 229-L sensor and the surrounding soil. Next, the technicians inserted the 229-L sensor into the cavity and backfilled the remainder of the slurry in the hole. As a result of this installation procedure, each sensor was in complete contact with the surrounding soil.

Following the installation of the 229-L sensors in the soil, technicians connected the wires in the trenches to the datalogger mounted on the Mesonet tower. Next, the technicians backfilled the trenches and permitted the vegetation to grow over the sensors and wires. Finally, QA personnel flagged the data from each 229-L sensor as erroneous for the initial 21 days of operation to allow the disturbed soil an initial recovery period to begin equilibrating with the surrounding environment. [For more information about how the Mesonet applies data quality flags to its processed data, see Shafer et al. (2000).]

3) WIRING ISSUES/ALUMINUM BLOCK

After burying the sensors, technicians wired the 229-L sensors into both a multiplexer, which is interfaced to a CR10X/CR23X datalogger, and a CE8 constant-current source. They connected two copper wires (heater wires) from each sensor to the CE8. The 229-L sensor has one copper–constantan thermocouple inside the hypodermic needle of the sensor that measures the temperature of the ceramic matrix. Unfortunately, when two different metals come into contact, a thermocouple forms. This creates a problem in the mux wiring because of the copper-diode contact and the constantan-diode contact. Thus, two new thermocouples form and create a potential source for inherent sensor error.

Mesonet technicians made a simple modification to remove the "extra" thermocouples from the wiring. The modification consisted of an aluminum block with five bored holes, a thermistor, and an extra copper wire. Mesonet technicians connected the copper wire and the constantan wire, creating a thermocouple, which allows both junctions at the mux to be copper. Because of the close proximity of the two copper connections, scientists assume both are at the same temperature. Thus, the connection of the wires creates no voltage difference. Technicians placed the new thermocouple within an aluminum block along with the thermistor.

The aluminum block allows for an approximately isothermal temperature profile to reduce any temperature difference between the thermocouple and the thermistor. Originally, scientists designed the thermistor to measure the temperature at the mux junction. However, this configuration ensured that the thermocouple and the thermistor were at the same temperature; thus, no voltage difference occurred. Oklahoma Mesonet personnel followed the same procedure for all four 229-L sensors, although only a single thermistor was needed within the aluminum block.

The accuracy of the temperature measurement in the 229-L sensor is equal to the type T thermocouple accuracy plus the isothermal block thermistor accuracy. For the type T thermocouple in the sensor's temperature range, the accuracy is $\pm$ 0.5°C. Campbell Scientific lists the accuracy of the T107 thermistor set used in the isothermal block as $<\pm 0.5$°C from $-35°$ to $+50$°C. This would provide an overall system error of $\sim\pm 1$°C. However, because calculations of all of the soil moisture variables are a difference in temperature rather than an absolute temperature, the magnitude of the sensor error does not directly translate into errors in the calculated variables.

4) SOIL CORE ANALYSIS

To determine the coefficients used to compute soil water content from a matrices potential (MP) measurement, researchers must determine a soil water retention curve (i.e., relationship between soil water potential and soil water content for a particular soil) from a soil core sample at each soil moisture sensor location. Because of the large number of sites and depths involved in the acquisition of Mesonet soil moisture data, it was not economically feasible to perform laboratory measurements of the soil water retention curve for all sites and depths. Scientists derived the soil water retention relationships used to compute soil water content (section 5b) using a combination of published empirical techniques. This approach utilized information on size distribution of soil particles available for all sites and depths and measured bulk density at some sites.

After collecting a soil sample, soil technicians determine its particle-size distribution and prepare the samples according to American Society for Testing and Materials (ASTM) D 421–85 (1985). An external soils laboratory performed hydrometer and wet sieving procedures, as described in ASTM D 422–63 (1963) and ASTM D 1140–92 (1992). Laboratory technicians entered the data into a spreadsheet, plotted the resulting particle-size distributions, calculated the percentages of sand, silt, and clay, and assigned the soil textural class according to the USDA classification system (i.e., the "soil texture triangle").

The Oklahoma Mesonet obtained bulk density measurements at some but not all sites. For those soil

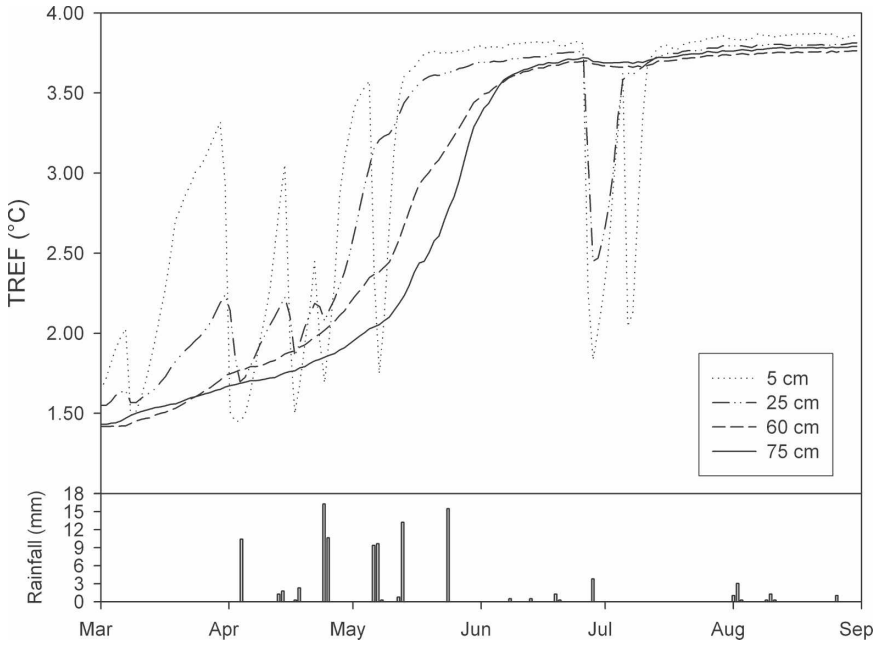

FIG. 4. Time series plot of the TREF and daily precipitation in Butler April–September 1998.

samples where measured bulk density was not available, Mesonet technicians estimated bulk density for different textural classes and depths in the soil profile using the methodology provided by Duke (1991). Soil texture information, soil coefficients, and other soil moisture–related information are included within the metadata of each Mesonet station.

4. Data quality

During operation at Mesonet sites, the sensor temperature (STxx) for each depth (xx) is measured. Next, the sensor is heated for 21 s. Following the heat pulse, the sensor temperature is measured again (FTxx). Sensor-specific coefficients are applied to the difference (ΔT) between STxx and FTxx to derive the reference temperature difference (TRxx; ΔT_{ref}).

a. Calculating TRxx coefficients

Each sensor has its own unique calibration coefficients that depend on the wet and dry values obtained in the laboratory. To remove the sensor-to-sensor variability, QA personnel apply a linear regression to normalize the response of an individual sensor to that of an idealized reference sensor having the following maximum and minimum ΔT values:

$$\Delta T_{\text{max}} = 3.96^{\circ}\text{C},$$

$$\Delta T_{\text{min}} = 1.38^{\circ}\text{C}.$$

The formulas [Eqs. (1) and (2)] used to calculate the slope (m) and intercept (b) coefficients are

$$m = \frac{(3.96 - 1.38)}{(\Delta T_{\text{max}} - \Delta T_{\text{min}})}, \quad (1)$$

$$b = 3.96 - (m \times \Delta T_{\text{max}}). \quad (2)$$

Once QA personnel determine the sensor's calibration coefficients, they record the sensor information on a calibration and tracking card and enter it into a database. Next, the sensor's response is normalized using Eq. (3):

$$\text{TRxx} = m \times T + b \ (\text{TRxx} = T_{\text{ref}}). \quad (3)$$

An example of ΔT_{ref} time series data is shown in Fig. 4. This figure of the sensor reference temperature (TREF) data from Butler, Oklahoma, from April to August 1998 shows a typical drying trend (i.e., increasing ΔT_{ref} values) seen at most sites. The shallower depths (5 and 25 cm) are much more variable and respond at a faster rate because of their proximity to the infiltrating precipitation and their larger ET rates during the growing season because of higher root density near the surface. The deeper depths (60 and 75 cm) respond more gradually to moistening (decreasing ΔT_{ref}) and drying (increasing ΔT_{ref}) and at times show almost no response to changing conditions seen at the shallower depths (e.g., mid-July of Fig. 4). Plants preferentially remove water near the surface first (energetically favorable) before tapping deeper layers, and un-

TABLE 1. Automated QA tests for soil moisture data collected by the Oklahoma Mesonet.

Test name	Description
Range	•If STxx or FTxx is below −30°C, the observation is flagged as "failure." If ST05 or FT05 is >55°C, the observation is flagged as failure. If ST25, ST60, ST75, FT25, FT60, and FT75 are >50°C, the observation is flagged as failure. •If the junction temperature is outside of the range –30°–55°C, the observation is flagged as failure.
Suspect calibration	•If TRxx is outside of the range 1.0°–4.1°C, the observation is flagged as failure. •If TRxx >1.0° but <1.38°C, the observation is flagged as "suspect" and the calibration coefficients are examined. •If TRxx <4.1° but greater than 3.96°C, the observation is flagged as suspect and the calibration coefficients are examined.
Step	•If TRxx at 5 cm increases by more than 0.75°C in 30 min, the observation is flagged as "warning." •If TRxx at 25, 60, or 75 cm increases by more than 0.50°C in 30 min, the observation is flagged as warning. •If TRxx at 5 cm decreases by more than 2.58°C in 30 min, the observation is flagged as warning. •If TRxx at 25 cm decreases by more than 2.5°C in 30 min, the observation is flagged as warning. •If TRx at 60 cm decreases by more than 2.0°C in 30 min, the observation is flagged as warning. •If TRxx at 75 cm decreases by more than 1.5°C in 30 min, the observation is flagged as warning. •If STxx or FTxx at 5 cm changes by more than 5°C in 30 min, the observation is flagged as warning. •If STxx or FTxx at 25, 60, or 75 cm changes by more than 3°C in 30 min, the observation is flagged as warning.
Freeze	•If STxx or FTxx is less than 1.25°C, the observation is flagged as suspect.

der high ET conditions plants can remove soil moisture before it infiltrates to the lower levels.

The ΔT_{ref} soil moisture variable is the official variable supported by the Oklahoma Mesonet. It has the virtue of requiring only a few simple calibrations and is the only soil moisture variable that is directly quality assured. However, other soil moisture variables, including volumetric water content and soil water potential, can be estimated using the quality assured ΔT_{ref} data. Because these other variables require more extensive calibrations and additional assumptions, the estimates include greater uncertainty than the ΔT_{ref} soil moisture variable. Information regarding the conversion of ΔT_{ref} to commonly used soil moisture variables is presented in section 5.

Over the course of the lifetime of a soil moisture sensor in the field, it may encounter drier or wetter conditions than observed in the laboratory (e.g., a sensor is immersed in saturated soil for a number of consecutive months). These extreme wet–dry observations in the field are even more appropriate than the laboratory wet–dry conditions for calculating the TRxx coefficients. Thus, if a particular sensor records a drier or wetter observation in the field than it displayed during its original laboratory calibration, QA personnel adjust the coefficients to incorporate the new wet or dry endpoint. QA personnel distribute and use the most recent coefficients of either kind (laboratory or field derived) in all further calculations of processed data. The updated coefficients are applied retroactively to all of the soil moisture data associated with that sensor.

b. Soil moisture QA procedures

A number of detailed, automated algorithms quality assure the ΔT_{ref} data (Table 1). In general, the algorithms ensure that 1) the data report within operational ranges, 2) the calibration coefficients are correct, and 3) frozen soil conditions are recognized. QA personnel investigate any failure of the automated tests. Information on problems verified by the QA personnel is subsequently submitted to a database and communicated to field technicians so that suspect sensors can be investigated and/or replaced. In some cases, the QA failure can be resolved by updating the sensor coefficients using field data. Quality assurance flags (Q) range in value from 0 to 9 (Shafer et al. 2000) and indicate good data, suspect data, sensor failure, uninstalled sensor, missing data, and other QA flags. When QA personnel assign a nonzero QA flag to an observation, the Mesonet's data processing system replaces the observations in the public data files with values indicating missing data, missing calibration values, no instrument installed, and quality assurance failures.

An example of data that failed an automated quality assurance test (the freeze test) and thus required manual inspection from QA personnel is shown in Fig. 5. The plot shows the 5-cm TREF data for Buffalo, Oklahoma, in 2005 during a period when the air and soil temperatures dropped below freezing. As such, the soil moisture sensor also froze, which resulted in dramatically decreased TREF values. In such cases, the automated quality assurance algorithms alert the QA

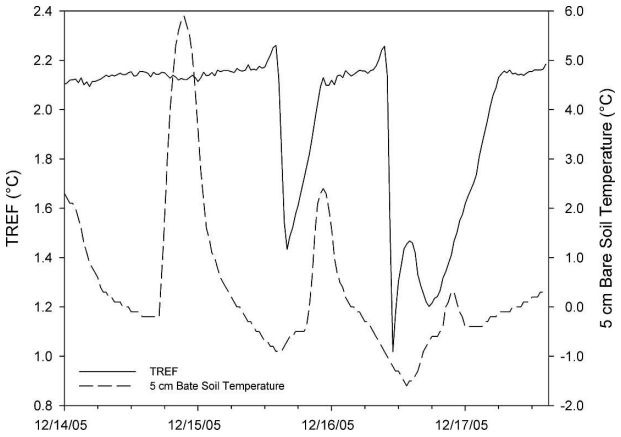

FIG. 5. The 5-cm sensor reference temperature (TR05) and 5-cm bare soil temperature (TB05) before quality assurance was applied for Buffalo in 2005. Observations became erratic on 15 Dec (and then dropped below the theoretical range of the measurement on 16 Dec) when soil temperatures decreased below freezing.

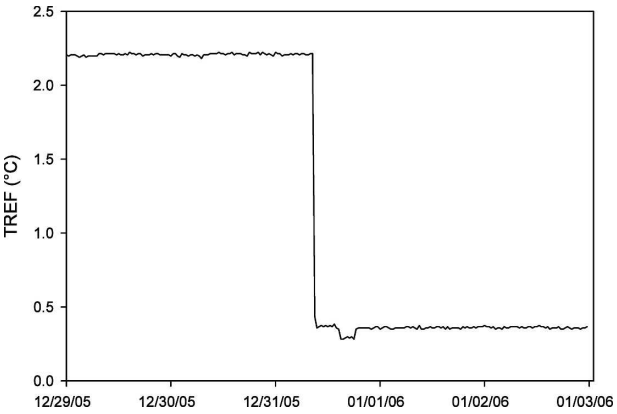

FIG. 6. The 25-cm TREF before quality assurance was applied for Kingfisher in late 2005 and early 2006. The sensor experienced a failure with its heating element.

personnel to the error so that the data can be flagged appropriately.

Another common QA problem with the 229-L sensor is displayed in Fig. 6. In this case, the heating element of the sensor failed at the Kingfisher, Oklahoma, site in late 2005. On 31 January 2005, the 25-cm reference temperature (TR25) abruptly dropped and resulted in erroneous data due to the failed sensor.

Because the performance of the 229-L sensor is dependent on the maintenance of hydraulic conductivity with the soil, sensors installed in soils with a high sand fraction are analyzed by Oklahoma Mesonet QA personnel to determine if the site's data should be flagged. Once analyzed, any relevant information is documented in the site's metadata.

At the end of each month, QA personnel analyze monthly averaged values of soil moisture data across Oklahoma. Through this process, they can detect subtle biases and manually process any erroneous data with additional QA flags. Further, QA personnel never alter observed data that fail the QA process in any form; the data only receives a QA flag in the database.

c. Errors associated with preferential flow

Basara and Crawford (2000) identified another possible source of sensor error. This error occurs because of the rapid wetting of the 60- and 75-cm sensors following a precipitation event caused by the preferential flow through the (refilled) trench dug to install the sensors. The sensors are operating properly, but the conditions measured by the sensors do not represent conditions in the surrounding undisturbed soil. Typically an extended period of weeks to months is required for the refilled trench to "heal" (i.e., the term applied to the development of contact between the disturbed soil in the trench and the undisturbed soil in which the sensor is placed). In some soils, it is nearly impossible to avoid the development of persistent macropores near the interface between the disturbed and undisturbed soils. Soils whose properties are conducive to the development of large macropores during drying (such as those with shrink–swell clays) are most susceptible to preferential flow problems.

The preferential flow errors most commonly occur when a heavy precipitation event follows an extended dry period (i.e., the soil is dry throughout the profile). The data pattern characteristic of this problem is an immediate wetting of the deeper (60 and 75 cm) sensors after a heavy rain event, followed by a rapid drying to the preprecipitation condition. The "normal" response for a recently wetted soil is an increase in soil moisture followed by a gradual decrease (i.e., over several days) as the soil dries. The preferential flow can disappear during a relatively wet period (the soil swells and fills the gap) but then reappear during another extended dry period.

Given these characteristics, it is difficult to develop an automated QA routine to detect these events. However, it should be noted that this problem is an anomaly in the standard operation of soil moisture sensors across Oklahoma. Of the over three million observations of soil moisture conditions collected between 1996 and 1999, the number of observations impacted by the preferential flow error accounted for less than one percent (Basara and Crawford 2000).

d. The importance of daily QA

Research quality soil moisture data are of critical importance to the Oklahoma Mesonet. In October 2002,

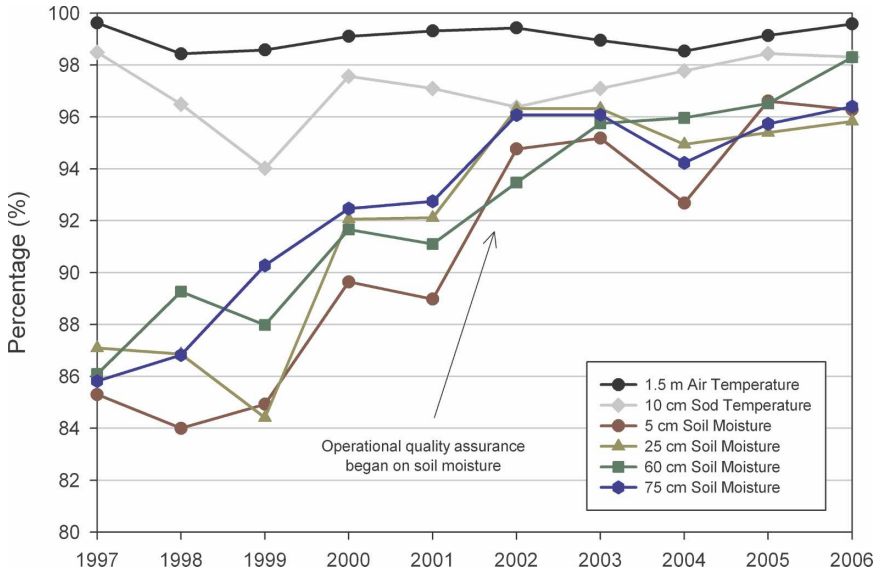

FIG. 7. Percentage of observations collected by the Oklahoma Mesonet that passed implemented QA procedures beginning with the deployment of the soil moisture sensors.

soil moisture became an operational parameter of the Oklahoma Mesonet. Prior to this designation, quality assurance of the soil moisture data was sporadic and focused on the generation of specific datasets. As such, sensor failures and the continuous collection of erroneous data were typically discovered following a significant time lag from when the problems began. However, with the designation as a core variable, QA procedures were conducted daily using a combination of automated routines and human inspection to determine erroneous observations and repair sensors with an increased response period.

Figure 7 shows the percentage of Oklahoma Mesonet soil moisture data that passed all quality assurance procedures since the deployment of the sensors. For comparison, the plot also displays two other core variables (air temperature at 1.5 m and soil temperature at 10 cm) that received daily QA during the entire period. Prior to 2002, the percentage of soil moisture observations that passed the QA procedures was significantly less than the other core variables of the Oklahoma Mesonet. However, once soil moisture became a core variable, the percentage increased to values consistent with other core variables collected by the Mesonet, and over 95% of the data collected was deemed as research quality in 2006.

5. Derived soil moisture variables

The calibrated ΔT_{ref} values support the calculation of several hydrological variables such as soil matrices potential (or soil water tension), soil water content, and fractional water index (FWI). Soil water content depends heavily on soil texture, while soil matrices potential (and soil water tension) is exponentially related to soil wetness. As a result, time series or mesoscale analyses based on these two variables are problematic, either across sites or even within the same profile.

a. Fractional Water Index

The FWI is a normalized value of the 229-L sensor response (Schneider et al. 2003). This unitless value ranges from 0.00 for very dry soil to 1.00 for soil at field capacity. The FWI is computed using Eq. (4):

$$\text{FWI} = \frac{\Delta T_d - \Delta T_{\text{ref}}}{\Delta T_d - \Delta T_w}, \tag{4}$$

where

FWI = fractional water index (unitless),
ΔT_{ref} = reference temperature difference,
ΔT_d = 3.96°C,
ΔT_{w} = 1.38°C.

The FWI is an ideal variable for mesoscale analyses and regional display purposes. It is not limited by varying soil texture at each site, it is a linear quantity with respect to the measured parameter (ΔT_{ref}), and it is easy to calculate. Therefore, it eliminates the complexities of matrices potential (an exponentially varying quantity) and water content (a soil-specific quantity of matrices potential that can vary even within a profile).

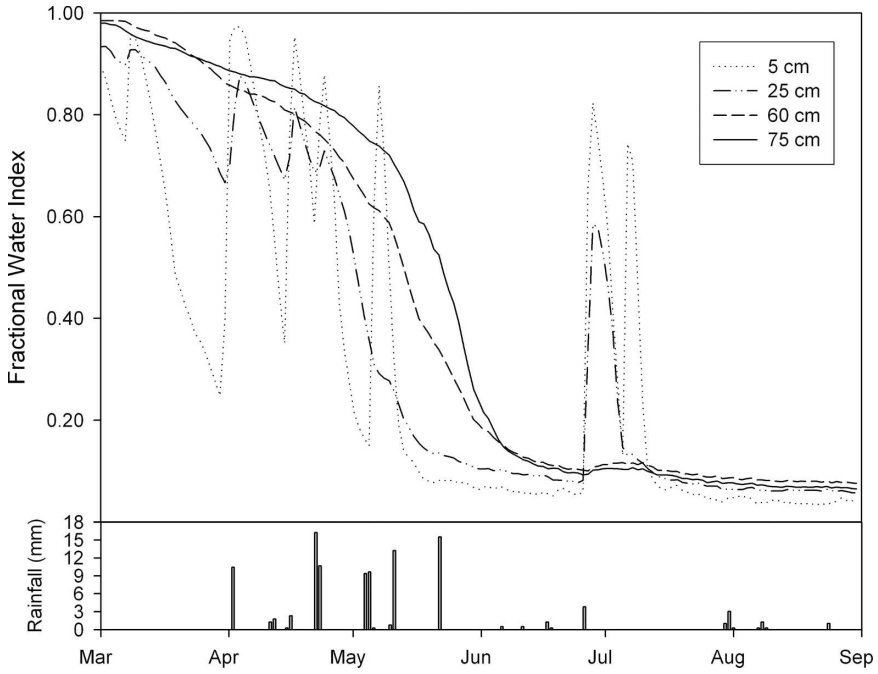

FIG. 8. Time series plot of the sensor FWI and daily precipitation in Butler April–September 1998.

While the FWI does not directly identify the soil water content or how vegetation will react to the soil moisture conditions, it is a relative measure of soil wetness that can be applied across an observing network. The range of 0 to 1 reflects the performance range of the 229-L sensor and extends from a state of low water availability to support transpiration to conditions slightly wetter than field saturation.

The example from April to September 1998 for Butler is plotted for the FWI in Fig. 8. Because soil characteristics are not used in calculating the FWI, the results are similar to the reference temperature (Fig. 4) and matrices potential plots (Fig. 9). In general, for public display, plots of fractional water index are the most intuitive to a nonscientific audience. As such, it is much easier to visualize the drying periods in May and June and the relative recharge of moisture in the shallow depths from the heavy rainfall in early July displayed in Fig. 8.

b. Soil matrices potential or water tension

Soil matric potential is the capillary force needed to retain water in the soil (Dingman 1994). Reece (1996) conducted a series of laboratory tests to determine the relationship between the 229-L sensor and matrices potential. He collected data from vacuum, pressure chamber, and tensiometer measurements and determined an empirical relationship between the 229-L sensors and matrices potential. Mesonet scientists performed similar research to determine a slightly modified empirical relationship between the 229-L sensors and matrices potential (Basara and Crawford 2000). Oklahoma Mesonet researchers further modified this empirical relationship to increase the accuracy of the relationship. The current relationship used (which defines the relationship between the calibrated ΔT_{ref} and matrices potential) is shown in Eq. (5):

See Addendum for updated formula (5)

where

MP = soil matrices potential (kPa),
WT = soil water tension (kPa),
a = calibration constant ($1.788^{\circ}\text{C}^{-1}$),
c = calibration constant (0.717 kPa),
ΔT_{ref} = reference temperature differential (°C).

Because of the sensitivity and range of the sensor, values of soil water potential greater than −8.5 kPa and less than −852 kPa are not accurate.

Soil matrices potential is an important quantity in soil physics because gradients in potential provide the "driving force" for soil water movement (Hillel 1980). In addition, soil matrices potential is critical to the agricultural community because it indicates the amount of force a plant must exert to extract water from the soil to support transpiration (Dingman 1994). Thus, the public

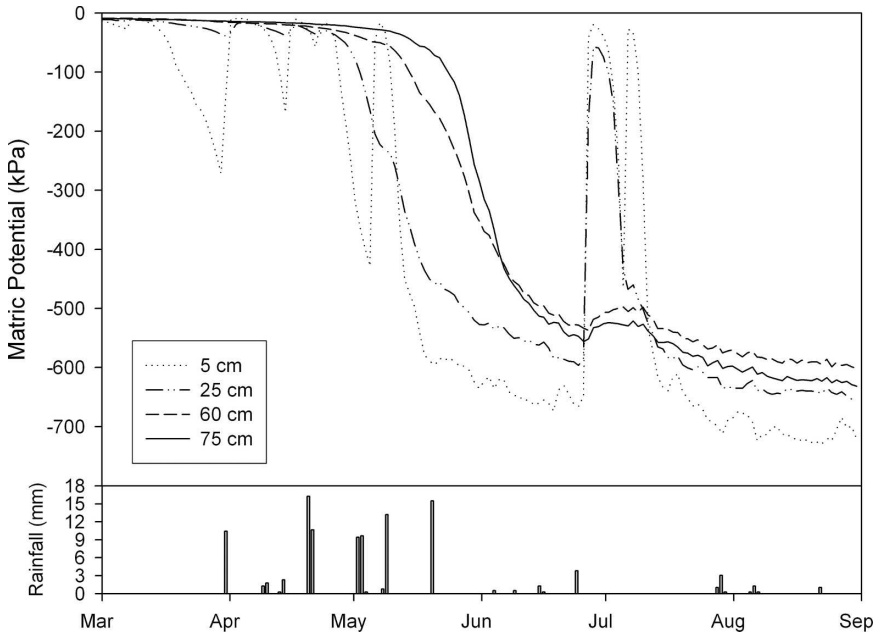

FIG. 9. Time series plot of the sensor soil MP and daily precipitation in Butler April–September 1998.

and the agricultural community can use real-time observations of soil matrices potential to quickly identify areas where plants may perish because of reduced potential (i.e., inadequate available moisture). However, because soil matrices potential varies exponentially with soil water content, it is difficult to interpolate precise values between observation locations in mesoscale analyses. Thus, users should interpret the potential estimates on depth-by-depth and site-by-site bases. A time series plot of the Butler soil matrices potential observations is depicted in Fig. 9. Note the inverse similarity in the pattern of the graph compared to ΔT_{ref} in Fig. 4 due to the indirect relationship between soil matrices potential and ΔT_{ref}.

c. Soil water content

Many numerical models in hydrology and the atmospheric sciences utilize mass balance as an important constraint, so they require volumetric soil water content as the measure of the soil moisture. Volumetric water content is defined as the total percent of water per volume of soil ($\text{cm}^3_{\text{water}}\ \text{cm}^{-3}_{\text{soil}}$; Dingman 1994) and can be determined from matrices potential measurements through the use of a soil water retention curve. Unfortunately, because of the large number of soil moisture sensors (at different sites and depths), it was not feasible to determine explicitly the soil water retention curve for each sensor depth in the laboratory. However, because Oklahoma Mesonet personnel collected detailed soil characteristics and collected or estimated soil bulk density measurements at each sensor location, estimated soil water retention curves were derived using the Arya and Paris (1981) methodology, which predicts the soil moisture characteristic, or water retention curve, from particle-size distribution and bulk density data. From this methodology, empirical coefficients α, n, WC_r, and WC_s are determined (Arya and Paris 1981), where

α = empirical constant (kPa^{-1}),
n = empirical constant (unitless),
WC_r = residual water content ($\text{cm}^3_{\text{water}}\ \text{cm}^{-3}_{\text{soil}}$),
WC_s = saturated water content ($\text{cm}^3_{\text{water}}\ \text{cm}^{-3}_{\text{soil}}$).

For each soil sample, researchers input the water content and water pressure values into the retention curve (RETC) program (van Genuchten et al. 1991), which then determines the coefficients. The RETC program requires estimates of the coefficients based on the texture of the soil sample. RETC fixes the initial value of the WC_s parameter at the saturated water content of the sample and does not allow it to vary during the RETC run. The saturated water content is determined by calculating the porosity of the sample based on the bulk density, assuming a particle density of 2.65 g cm^{-3} and that the entire pore space is filled with water. With WC_s fixed, only the values of WC_r, α, and n are determined by the program. Initial values for these three coefficients for each soil textural class are provided by Rawls et al. (1982).

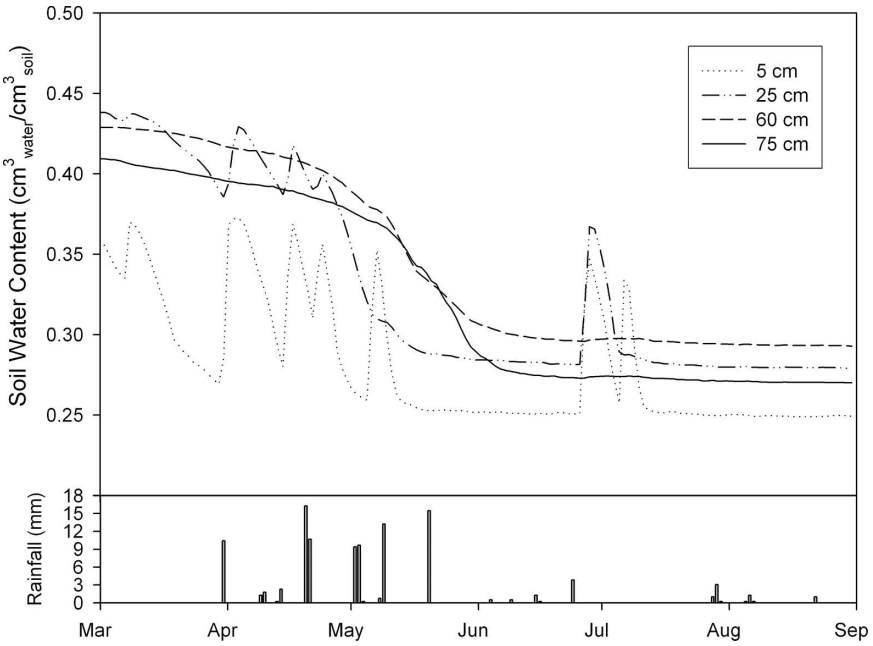

FIG. 10. Time series plot of the sensor soil WC and daily precipitation in Butler April–September 1998.

The van Genuchten (1980) method subsequently uses the empirical coefficients α, n, WC_r, and WC_s to determine volumetric water content from matrices potential values. As such, this method is utilized by the Oklahoma Mesonet to compute the volumetric water content and is shown in Eq. (6):

See Addendum for correct formula (6)

where

WC = soil water content on a volume basis (cm^3_{water} cm^{-3}_{soil}).

The soil water content values from April to August 1998 for Butler are depicted in Fig. 10. Because each soil depth at Butler has unique soil properties, the moist and dry "baselines" for each depth also differ. For instance, the 75-cm depth is composed of silty clay loam, which is capable of drying to a lower volumetric content than can the shallower depths.

Because laboratory analyses of soil water retention curves were not conducted as part of the soil moisture sensor installation within the Oklahoma Mesonet, the relative errors between the derived (estimated) retention curves and similar laboratory analyses are not known. However, to quantify the uncertainty in the soil water content estimates [see WC in Eq. (6)] produced across Oklahoma, Mesonet researchers conducted independent field measurements of soil water content at numerous locations. Two established measurement techniques were used for conducting the experiment.

The first method (referred to as gravimetric sampling) involves the destructive field sampling of soil cores in the proximity of the Mesonet stations. Researchers extracted soil cores approximately 2 cm in diameter and 5 cm in length (centered at the depth of the sensors) from the soil profile at 20 different Mesonet sites over a range of soil moisture conditions; a total of 264 gravimetric samples of soil moisture were collected. They weighed the extracted cores before and immediately after drying the cores in an oven. Once this process was completed, they compared the volumetric water (as calculated by multiplying the percent water by weight and the soil bulk density) with the estimates derived from the 229-L sensor measurements. To increase the representativeness of the field samples and to minimize potential error during collection, three replicate samples acquired within several meters of one another were processed and averaged by researchers to obtain a single value used in the intercomparison analysis. The comparison between the field measurements acquired using the gravimetric technique and the 229-L sensor estimates at corresponding times and depths is shown in Fig. 11. The RMSE between the destructive field measurements and the 229-L sensor estimates was 0.066 cm^3 cm^{-3}.

The second method for obtaining field measurements

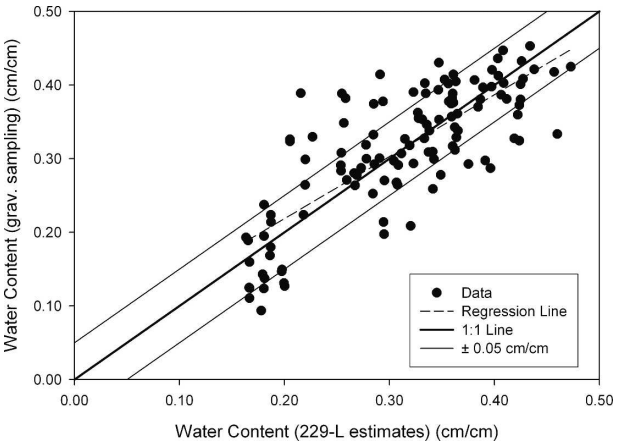

FIG. 11. Water content values measured with the destructive field sampling vs water content estimates derived from 229-L sensor measurements. These points represent sampling locations at 20 different Mesonet sites.

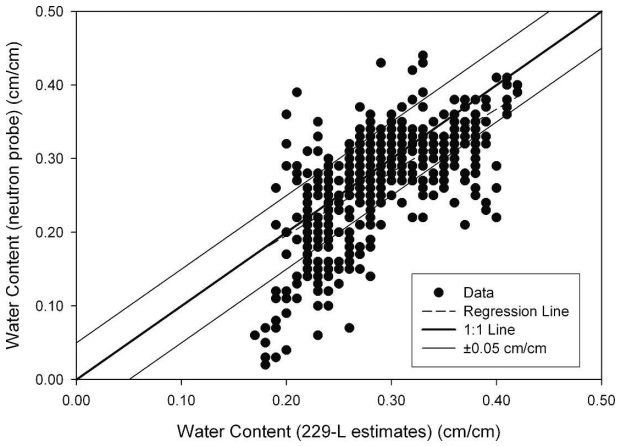

FIG. 12. Volumetric water content values measured with the neutron probe vs volumetric water content values from the sensors.

utilized neutron scattering techniques, which have a long history in the field of soil physics (Holmes 1956; van Bavel 1963). This method utilizes a radioactive element lowered into a preinstalled access tube in the soil. Neutrons are released from the radioactive source at a predetermined depth and the scatter of the neutrons is measured. The amount of neutron scatter is a function of hydrogen atoms in the soil and a direct indication of the soil water content. Still, disadvantages exist to using the neutron scattering method to measure soil moisture. For example, the sensors need to be handled with caution because of the radioactive components of the devices; they are inaccurate near the land surface, and they cannot be left unattended (Ould Mohamed et al. 1997). Data were obtained by this technique at the 25-, 60-, and 75-cm depths at 45 different sites for a total of 644 independent measurements.

The comparison between field measurements with the neutron probe (NP) and the estimates derived from the 229-L sensor measurements at corresponding depths and times is shown in Fig. 12. The RMSE between the neutron probe measurements and the 229-L sensor estimates was 0.052 cm^3 cm^{-3}. Further, while there appeared to be a tendency for the values derived from the 229-L sensor to be slightly wetter than the NP values, many of the overestimated data points correspond to dry conditions, particularly less than 0.15 cm^3 cm^{-3}.

There are several spatial sampling issues associated with the comparison of any two different techniques for measuring soil water content that must be considered. The sensors are never perfectly collocated and thus local-scale soil heterogeneity can influence comparisons between different techniques. This is usually somewhat addressed with sample replicates; however, only a single 299-L sensor exists at each site and depth. Sampling volume also varies somewhat among sensors and field measurement techniques; the field techniques discussed here are sensitive to a slightly larger volume of soil surrounding the central measurement point than are the 229-L sensors. Further, both gravimetric sampling (which, when properly conducted, is as close to "truth" as can be measured in the field) and neutron probe measurements include inherent error. This is particularly true for gravimetric samples collected near the surface during drying periods where gradients of soil water may exist within the integrated layer. Given these sampling issues and the typical range of RMSE values associated with soil moisture intercomparisons, the RMSE values provided represent a reasonable range of the accuracy of the WC measurements derived with the 229-L sensors. As such, the maximum uncertainty of the derived soil water content from the 229-L sensors installed across the Oklahoma Mesonet is approximately 0.05 cm^3 cm^{-3}.

6. Discussion

a. Measurement representativeness

Because the 229-L sensor represents a point measurement, data users must be aware of the spatial and temporal limitations of the observations. Soil texture and organic properties vary significantly both horizontally and vertically (Hills and Reynolds 1969; Bell et al. 2003; Nyberg 1996; Famiglietti et al. 1999). As such, the magnitude of the soil water content varies because of the diverse physical characteristics of the soil. Basara and Crawford (2002) investigated the variability of soil

water content and soil texture at the Norman, Oklahoma, Mesonet site. They collected approximately 3000 gravimetric samples from 12 locations within 20 m of the site at varying depths from 0 to 80 cm over a 3-month period. The results of the gravimetric water content–textural class analysis demonstrated that 1) the typical observed range of volumetric water content at any given depth interval (e.g., 0–5, 5–10 cm, etc.) was approximately ± 0.05 cm^3 cm^{-3} and decreased slightly with depth; 2) the horizontal soil texture varied slightly but soil texture changed significantly with depth (e.g., silt loam at 0–30 cm and clay loam from 30–80 cm); and 3) the soil water content values produced by the 229-L sensors were within the natural variability of the observed conditions.

Unfortunately, such studies require extensive resources to conduct and are cost prohibitive across a network of over 100 stations. The outcome of the Basara and Crawford (2002) analysis revealed that while the 229-L sensor observed soil water content values representative of the conditions surrounding the site, significant variability existed in the magnitude of water content at the location. However, the temporal correlation between the automated observations and the field sample was quite large, providing some confidence that the relative changes in soil water are a more accurate signal. Oklahoma Mesonet soil moisture data are better suited to studies focused on long-term soil moisture conditions and observed temporal variability on the mesoscale (e.g., Luo et al. 2003; Illston et al. 2004).

b. Soil moisture products

OCS provides quality assured soil moisture data from the Oklahoma Mesonet to the public via Internet resources and archived capacities (McPherson et al. 2007). The Oklahoma Mesonet public products site (http://www.mesonet.org/public) includes near-real-time and historical soil moisture products in the form of interactive maps and graphs. These products are found within the Interactive Products section of the site. Additionally, the public can use OCS's WxScope Plugin software (Wolfinbarger et al. 1998) to view Web-based soil moisture products.

The Web site includes maps that display daily averages of categorized matrices potential and the fractional water index at 5, 25, 60, and 75 cm. Maps displaying the most recent data are available via direct links on the Web site. In addition, users can create custom maps from historical data dating from 1 January 1997. Time series graphs of soil moisture products are also available. The standard graph displays the fractional water index and volumetric water content at all depths from a single site over the past 30 days. Users can create custom graphs from the historical archive starting on 1 January 1997. These products can display up to 90 days of data from a single site. Instead of soil matrices potential observations, the Oklahoma Mesonet plots soil matrices potential categories.

7. Conclusions

The Oklahoma Mesonet added soil moisture sensors to over 100 stations between 1996 and 1999. Data are collected using the Campbell Scientific 229-L sensor integrated into the Oklahoma Mesonet infrastructure and quality assured using a combination of automated algorithms and human inspection. This project also demonstrated the importance of operational QA regarding the data collected, whereby the percentage of observations that passed the QA procedures significantly increased once daily QA was applied. The QA procedures are applied to data directly collected from the 229-L sensors. As such, derived soil moisture variables including the FWI, soil matrices potential, and soil water content include the base QA applied to the sensor output. For soil water content, independent measurements were collected via gravimetric sampling and neutron probe samples and were compared to the derived values from the 229-L sensor measurements. The results yielded RMSE differences of 0.066 and 0.052 cm^3 cm^{-3} for the gravimetric and neutron probe analyses. Thus, the maximum uncertainty of the derived soil water content from the 229-L sensors installed across the Oklahoma Mesonet is approximately 0.05 cm^3 cm^{-3}.

The deployment of soil moisture sensors across Oklahoma has enhanced the observational capabilities of the Mesonet as well as benefited research projects focused on mesoscale drought and land–atmosphere interactions. The need for long-term, research-quality observations of soil moisture will continue, and as such, the collocated observations of soil moisture and atmospheric variables at Oklahoma Mesonet stations will provide extremely valuable datasets.

Acknowledgments. The installation of the Oklahoma Mesonet's soil moisture sensors was made possible, in part, by an NSF-EPSCOR grant (Project Number EPS9550478) and an NSF MRI grant (ATM-9724594). Continued funding for maintenance of the network is provided by the taxpayers of the State of Oklahoma. In addition, support from the NOAA Office of Global Programs (NOAA Grant Number NA17RJ1227) was instrumental in the development of research-quality datasets. The authors thank James Kilby, David Grims-

ley, Bill Wyatt, Ken Meyers, Kris Kesler, and numerous staff members of the Oklahoma Climatological Survey for their professional assistance in maintaining the Oklahoma Mesonet. In addition, the authors would like to acknowledge the efforts of Jeanne Schneider and Michael Cosh, whose insights improved the quality of the manuscript.

REFERENCES

Anthes, R. A., 1984: Enhancement of convective precipitation by mesoscale variation in vegetative covering in semiarid regions. *J. Climate Appl. Meteor.,* **23,** 541–554.

Arya, L. M., and J. F. Paris, 1981: A physicoempirical model to predict the soil moisture characteristic from particle-size distribution and bulk density data. *Soil Sci. Soc. Amer. J.,* **45,** 1023–1030.

Basara, J. B., 1998: The relationship between soil moisture variation across Oklahoma and the physical state of the near-surface atmosphere during the spring of 1997. M.S. thesis, School of Meteorology, University of Oklahoma, 192 pp.

——, and T. M. Crawford, 2000: Improved installation procedures for deep layer soil moisture measurements. *J. Atmos. Oceanic Technol.,* **17,** 879–884.

——, and K. C. Crawford, 2002: Linear relationships between root-zone soil moisture and atmospheric processes in the planetary boundary layer. *J. Geophys. Res.,* **107,** 4274, doi:10.1029/2001JD000633.

Bell, T. L., and P. K. Kundu, 2003: Comparing satellite rainfall estimates with rain gauge data: Optimal strategies suggested by a spectral model. *J. Geophys. Res.,* **108,** 4121, doi:10.1029/2002JD002641.

Betts, A. K., and J. H. Ball, 1995: The FIFE surface diurnal cycle climate. *J. Geophys. Res.,* **100,** 25 679–25 694.

Brock, F. V., K. C. Crawford, R. L. Elliott, G. W. Cuperus, S. J. Stadler, H. L. Johnson, and M. D. Eilts, 1995: The Oklahoma Mesonet: A technical overview. *J. Atmos. Oceanic Technol.,* **12,** 5–19.

Brubaker, K. L., and D. Entekhabi, 1996: Analysis of feedback mechanisms in land-atmosphere interaction. *Water Resour. Res.,* **5,** 1343–1358.

——, ——, and P. S. Eagleson, 1993: Estimation of continental precipitation recycling. *J. Climate,* **6,** 1077–1089.

Delworth, T., and S. Manabe, 1989: The influence of soil wetness on near-surface atmospheric variability. *J. Climate,* **2,** 1447–1462.

——, and ——, 1993: Climate variability and land surface processes. *Adv. Water Resour.,* **16,** 3–20.

Dingman, S. L., 1994: *Physical Hydrology*. Maxwell Macmillan International, 575 pp.

Duke, H. R., 1991: Scheduling irrigations: A guide for improved irrigation water management through proper timing and amount of water application. U.S. Department of Agriculture, Agricultural Resource Service and Soil Conservation Service Colorado Tech. Bull.

Emanuel, K., and Coauthors, 1995: Report of the first prospectus development team of the U.S. Weather Research Program to NOAA and the NSF. *Bull. Amer. Meteor. Soc.,* **76,** 1194–1208.

Enger, L., and M. Tjernstrom, 1991: Estimating the effects on regional precipitation climate in semiarid regions caused by an artificial lake using a mesoscale model. *J. Appl. Meteor.,* **30,** 227–250.

Entekhabi, D., and Coauthors, 1999: An agenda for land surface hydrology research and a call for the Second International Hydrological Decade. *Bull. Amer. Meteor. Soc.,* **80,** 2043–2058.

Famiglietti, J. S., and Coauthors, 1999: Ground-based investigation of soil moisture variability within remote sensing footprints during the Southern Great Plains 1997 (SGP97) Hydrology Experiment. *Water Resour. Res.,* **35,** 1839–1852.

Hillel, D., 1980: *Environmental Soil Physics*. Academic Press, 771 pp.

Hills, T. C., and S. G. Reynolds, 1969: Illustrations of soil moisture variability in selected areas and plots of different sizes. *J. Hydrol.,* **8,** 27–47.

Holmes, J. W., 1956: Calibration and field use of the neutron scattering method of measuring soil water content. *Aust. J. Appl. Sci.,* **7,** 45–58.

Illston, B. G., J. B. Basara, and K. C. Crawford, 2004: Seasonal to interannual variations of soil moisture measured in Oklahoma. *Int. J. Climate,* **24,** 1883–1896.

Lanicci, J. M., T. B. Carlson, and T. T. Warner, 1987: Sensitivity of the Great Plains severe-storm environment to soil-moisture distribution. *Mon. Wea. Rev.,* **115,** 2660–2673.

Luo, L., and Coauthors, 2003: Validation of the North American Land Data Assimilation System (NLDAS) retrospective forcing over the southern Great Plains. *J. Geophys. Res.,* **108,** 8843, doi:10.1029/2002JD003246.

McPherson, R. A., and Coauthors, 2007: Statewide monitoring of the mesoscale environment: A technical update on the Oklahoma Mesonet. *J. Atmos. Oceanic Technol.,* **24,** 301–321.

Nyberg, L., 1996: Spatial variability of water content in the covered catchment at Gardsjon, Sweden. *Hydrol. Processes,* **10,** 89–103.

Ould Mohamed, S., P. Bertuzzi, A. Bruand, L. Raison, and L. Bruckler, 1997: Field evaluation and error analysis of soil water content measurement using the capacitance probe method. *Soil Sci. Amer. J.,* **61,** 399–408.

Rawls, W. J., D. L. Brakensiek, and K. E. Saxton, 1982: Estimating soil water properties. *Trans. Amer. Soc. Agric. Eng.,* **25,** 1316–1320, 1328.

Reece, C. F., 1996: Evaluation of a line heat dissipation sensor for measuring soil matric potential. *Soil Sci. Soc. Amer. J.,* **60,** 1022–1028.

Schneider, J. M., D. K. Fisher, R. L. Elliott, G. O. Brown, and C. P. Bahrmann, 2003: Spatiotemporal variations in soil water: First results from the ARM SGP CART network. *J. Hydrometeor.,* **4,** 106–120.

Segal, M., and R. W. Arritt, 1992: Nonclassical mesoscale circulations caused by surface sensible heat-flux gradients. *Bull. Amer. Meteor. Soc.,* **73,** 1593–1604.

——, ——, C. Clark, R. Rabin, and J. Brown, 1995: Scaling evaluation of the effects of surface characteristics on the potential for deep convection over uniform terrain. *Mon. Wea. Rev.,* **123,** 383–400.

Shafer, M. A., C. A. Fiebrich, D. S. Arndt, S. E. Fredrickson, and T. W. Hughes, 2000: Quality assurance procedures in the Oklahoma Mesonetwork. *J. Atmos. Oceanic Technol.,* **17,** 474–494.

Starks, P. J., 1999: A general heat dissipation sensor calibration equation and estimation of soil water content. *Soil Sci.,* **164,** 655–661.

van Bavel, C. H. M., 1963: Neutron scattering measurements of soil moisture: Development and current status. *Proc. Int. Symp. on Humidity and Moisture,* Washington, DC, 171–184.

van Genuchten, M. T., 1980: A closed-form equation for predicting the hydraulic conductivity of unsaturated soils. *Soil Sci. Soc. Amer. J.,* **44,** 892–898.

——, F. J. Leij, and S. R. Yates, 1991: The RETC code for quantifying the hydraulic functions of unsaturated soils. U.S. Environmental Protection Agency Rep. EPA/600/2-91/065, 93 pp.

Wolfinbarger, J. M., R. A. Young, and T. B. Stanley, 1998: Delivering real-time interactive data from the Oklahoma Mesonet via the World Wide Web. Preprints, *14th Int. Conf. on Interactive Information and Processing Systems for Meteorology, Oceanography, and Hydrology,* Phoenix, AZ, Amer. Meteor. Soc., 213–217.

Zdunkowski, W. G., J. Paegle, and J. P. Reilly, 1975: The effect of soil moisture upon the atmospheric and soil temperature near the air-soil interface. *Arch. Meteor. Geophys. Bioklimatol.,* **24,** 245–268.

Addendum

Formula (5) was updated as the resulted of research published in:

Zhang, Y., T. E. Ochsner, C. A. Fiebrich and B. G. Illston, 2019: Recalibration of Sensors in One of The World's Longest Running Automated Soil Moisture Monitoring Networks. Soil Science Society of America Journal, 83 (4), 1003-1011. (DOI: 10.2136/sssaj2018.12.0481).

It should now read:

$\mathrm{MP} = -2083/(1+\exp(-3.35(\Delta T_{\mathrm{ref}}-3.17)))$; (WT = -MP)

Formula (6) should read as follows:

$$WC = WC_r + \frac{WC_s - WC_r}{\left(1+\left(-a \cdot MP\right)^n\right)^{\left(1-\frac{1}{n}\right)}}$$